

Behavior of a Cold Ion Plasma in a Toroidal Octupole*

J. C. SPROTT

Department of Physics, University of Wisconsin, Madison, Wisconsin 53706
(Received 6 October 1969)

By raising the background hydrogen gas pressure to $\sim 10^{-4}$ Torr and injecting 10–100 kW of 700–9000 MHz microwave power for ~ 100 μ sec, an afterglow plasma with $n \sim 10^9$ – 10^{11} cm^{-3} and $kT_i < kT_e \sim 1$ eV can be produced in the Wisconsin toroidal octupole. The particle lifetime is ~ 3 msec, or somewhat longer than for a hot ion, gun injected plasma, and most ($\sim 80\%$) of the plasma is lost to the hoops. The electron temperature decays rapidly as a result of inelastic electron–neutral collisions. By changing the magnetic field strength and microwave frequency, the density distribution can be varied, and a variety of fluctuations produced. These fluctuations do not appear to be an important source of plasma loss.

I. INTRODUCTION

Most previous studies of plasma confinement in the Wisconsin toroidal octupole have used a hot ion ($kT_i \sim 40$ eV) plasma produced by a conical z -pinch gun outside the magnetic field.^{1,2} Early measurements¹ showed that the plasma was quiescent and indicated a loss rate for ions that was consistent with thermal flow to hoop supports and probes. Later measurements³ of direct particle loss showed that most of the loss was to the hoops and that the supports contributed only a minor part of the total loss.

Plasmas produced by microwave heating at the electron cyclotron frequency are of interest because of their much lower ion temperature and because the comparison of confinement in the Wisconsin octupole with other multipole experiments⁴ using cold ion plasmas is facilitated. It was expected that if confinement is limited by the flow of ions to the supports or by the small number of gyroradii between the hoops and walls, that a cold ion plasma would exhibit significantly better confinement properties. That this was not the case provided further evidence for the existence of some additional, unexplained loss mechanism. The microwave produced plasma also provides an opportunity to vary the density distribution by changing the location of the resonance zones and thereby producing a variety of fluctuations.

Two types of microwave heating experiments have been performed on the toroidal octupole. The first type consists of injecting a gun plasma into the field at low background pressure ($\sim 10^{-6}$ Torr), allowing it to reach a quiescent state, and then injecting a pulse of microwaves into the cavity. The average electron energy is observed to rapidly reach equilibrium at 100 eV–1 keV where the heating rate is balanced by the loss of energetic electrons to

obstacles in the plasma. When the microwaves are turned off, the electron energy rapidly (~ 100 μ sec) returns to near its original value. These experiments, along with a theoretical model for calculating the heating rate in an arbitrary, nonuniform magnetic field, are described in another paper.⁵

The second type of experiment consists of raising the background hydrogen gas pressure to $\sim 10^{-4}$ Torr and injecting microwaves with no preionization. The gas is partly ionized and heated by the microwaves, producing a cold ion ($T_i < T_e$), warm electron ($kT_e \sim 1$ eV) plasma with a density of 10^9 – 10^{11} cm^{-3} in the afterglow. An electrostatic energy analyzer places an upper limit of ~ 1 eV on the ion temperature. This paper describes the behavior of this cold ion plasma.

Microwave power is produced by pulsed magnetrons operating at frequencies of 700, 1300, 3250, 5280, and 9000 MHz with peak output powers of 10–100 kW and pulse lengths up to 144 μ sec. The power is carried through a waveguide to a hole in the vacuum tank wall at the higher frequencies, or through a coaxial line to a $\frac{1}{4}$ wave antenna inside the cavity at low frequencies.

II. PLASMA MOTION

It has previously been shown⁵ that microwave heating is strongly localized in regions where $\nabla_{\parallel} B = 0$ at resonance. For example, in Fig. 1, which shows a flux plot of the toroidal octupole, the microwave frequency could be chosen so that resonance occurs on the surface $B_0 = 1$ kG. Maximum heating would then occur of flux surfaces that are tangent to the resonance surface at the minimum of the local mirrors. The plasma is created in these resonance zones and spreads quickly along the field lines, so that the density distribution in flux space is peaked on either side of the separatrix.

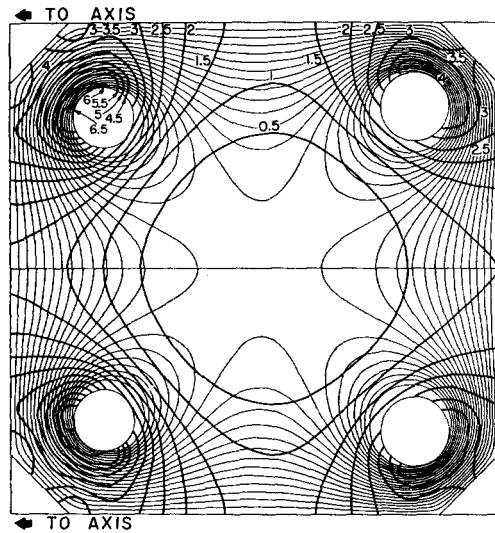


FIG. 1. Computer calculated magnetic flux plot of the octupole field. The light lines are magnetic field lines, numbered from $\psi = -5$ at the hoops to $\psi = +5$ at the walls. The heavy lines are contours of constant magnetic field strength.

Figure 2 shows a profile of ion saturation current to a floating double probe for a scan from the inside wall along the midplane to the $B = 0$ axis and then diagonally up to an inner hoop. The times are measured after the beginning the 100 μsec microwave pulse. Resonance is at $B_0 = 1.15$ kG. At 60 μsec (during the heating pulse) the ion saturation current is strongly peaked off the separatrix, producing pressure gradients opposite to those required for magnetohydrodynamic stability. Such an inverted gradient can be stable provided⁶

$$pV'' \frac{d}{d\psi} \ln(pV'^{5/3}) > 0.$$

For $T_e = \text{const}$, this condition is equivalent to requiring that the slope of the ion saturation current on a log scale be less than the slope of the function $V'^{-5/3}$

$$\left| \frac{d \ln I_{oi}}{d\psi} \right| < \left| \frac{d \ln V'^{-5/3}}{d\psi} \right|.$$

In Fig. 2, it is clear that the distribution at 60 μsec exceeds the stability limit. Large, low-frequency electric fields are observed which cause the plasma to collapse toward the separatrix producing a relatively flat density distribution by 200 μsec . The ion saturation current thereafter decays slowly with relatively little change in spatial distribution.

Since the perpendicular component of the rf field in the resonance region varies with azimuth, it is not surprising that azimuthal density variations of

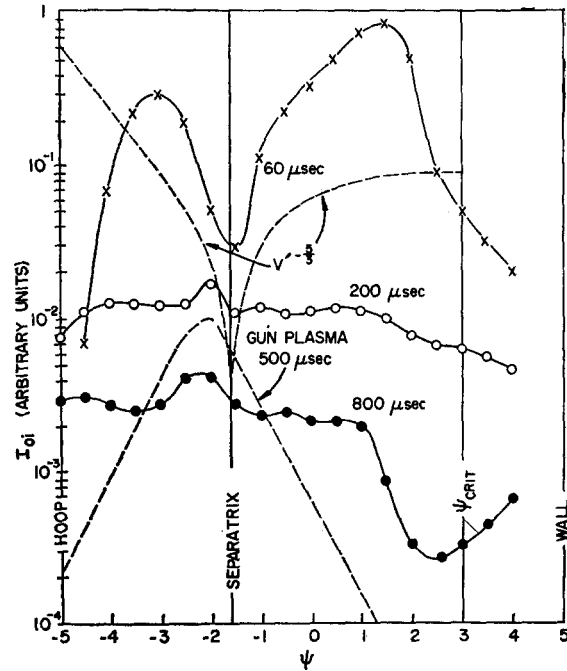


FIG. 2. Ion saturation current profiles in ψ -space for various times after the beginning of a 100 μsec pulse of 3250 MHz microwaves.

about a factor of 2 are observed in the afterglow. These variations are smallest on the separatrix and persist throughout the life of the plasma. To a good approximation, the density is constant on a magnetic field line.

Oscillographs summarizing the gross behavior of the plasma are shown in Fig. 3. Figures 3(a) and (b) show the large ion saturation current, floating potential, and azimuthal electric field in the resonance region during heating. Figure 3(c) indicates that after the heating phase the ion saturation current and floating potential on the $B = 0$ axis decay slowly in time with no observable fluctuations. Figures 3(d) and (e) show that at the edges of the plasma near the hoops and wall there are appreciable fluctuations in the floating potential. These phenomena will be discussed in more detail in Sec. V.

By changing the magnetic field strength and microwave frequency, a variety of density distributions can be obtained. One interesting case is produced when resonance occurs at $B_0 = 5$ in Fig. 1. This contour produces plasma only on the field lines $-5 < \psi < 0$ near the inner hoops. Resonance does not occur on the lines between the separatrix and the outer hoops, and so a scan between the wall and an outer hoop should show the initial density strongly peaked near the separatrix in the region $-1.6 < \psi < 0$.

Figure 4 shows the ion saturation current for such a scan produced by a 144 μsec pulse of 9000 MHz microwaves 1.2 msec after the beginning of the 5 msec half-sine-wave magnetic field pulse. The

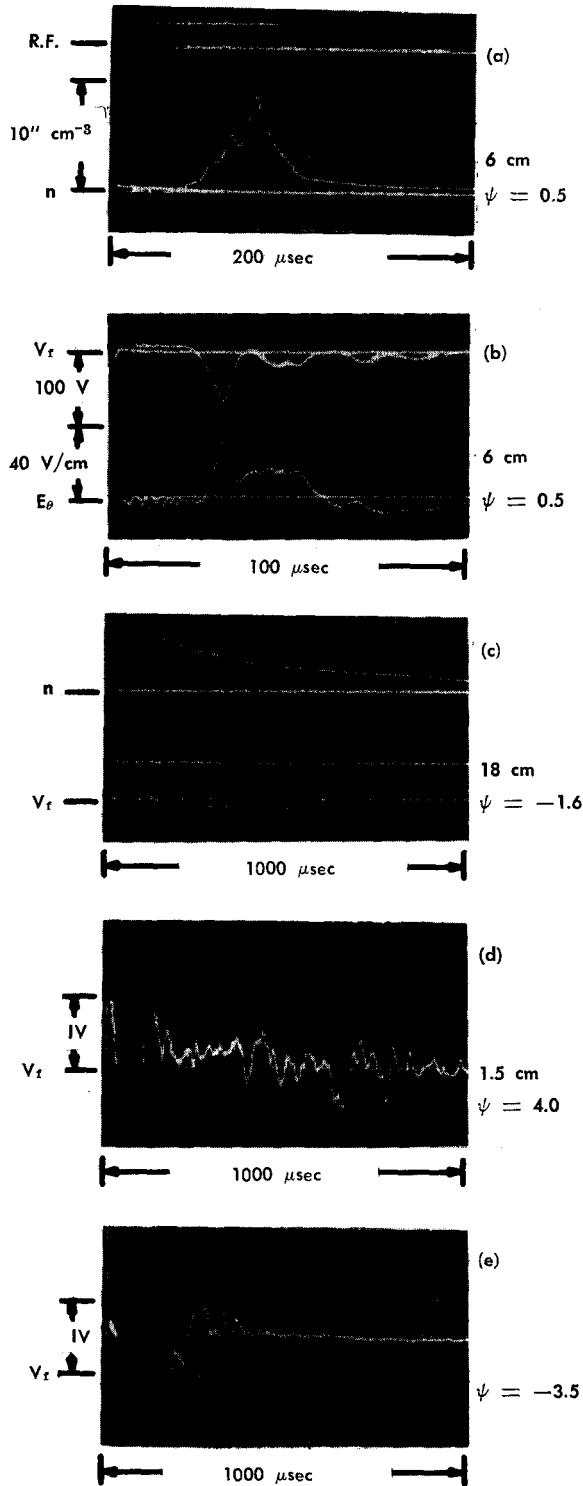


Fig. 3. Oscillographs summarizing the gross behavior of the plasma.

distribution at 1.5 msec is sharply peaked near the separatrix, although even at this early time an appreciable amount of plasma has diffused toward the hoop. This distribution is interesting because it resembles the distribution for the gun injected plasma. By 2.5 msec the density peak has moved significantly toward the hoop. This motion is due in part to the inductive electric field caused by the rising magnetic field. This effect, by itself, would cause a distribution peaked on the separatrix ($\psi = 1.6$) at 1.5 msec to evolve into a distribution peaked at $\psi = -2.3$ at 2.5 msec. Figure 4 indicates, that in addition to this field line motion, a considerable diffusion is present. By 3.5 msec the field is decreasing sharply, leaving a dip on the separatrix where a small number of particles fill a large volume. By 4.5 msec, the plasma is moving rapidly to the walls.

Lencioni⁷ has treated theoretically the problem of the evolution of a density profile in the presence of a changing magnetic field for the case in which the plasma motion is flux invariant. In the zero gyroradius limit, his results indicate that the density should fall to zero on the separatrix and become infinite on the field line that was initially the separatrix. Experiments⁷ on the gun injected plasma indicate a tendency toward this behavior but greatly reduced by the finite ion gyroradius and other effects. It was hoped that the microwave plasma with its small gyroradii ($\Delta\psi < 0.1$) would strongly exhibit the effects of field line motion, but apparently other processes such as fluctuating electric fields cause diffusion of the plasma across the field.

Although a density distribution initially peaked near the separatrix is expected to be stable against simple interchange instabilities, one might argue

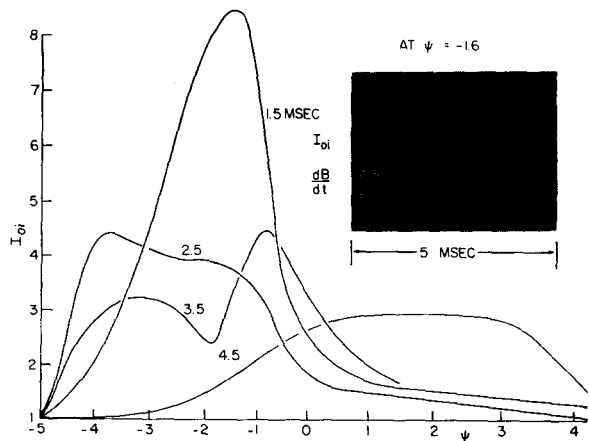


Fig. 4. Ion saturation current profiles in ψ space for various times after the beginning of the magnetic field pulse. The 144 μsec pulse of 9000 MHz microwaves begins at 1.2 msec.

that since the plasma is produced in places where the magnetic field strength is comparable to the magnetic field at the surface of the hoops and walls, it is energetically possible for the plasma to escape from the field. To test the validity of this argument, the plasma produced by 700 MHz microwaves was examined. For this case, resonance occurs on a circle of radius 7.5 cm ($B_0 = 0.25$ kG) at a place where $B_{\text{hoop}}/B_0 \approx 8$ for the outer hoop. The ion saturation current distribution was measured to determine the evolution of the density profile. Initially, the plasma is well confined near the separatrix, but as time goes on a rapid diffusion toward the hoops and wall is observed. The evolution of the profile looks quite similar to the 9000 MHz case of Fig. 4 indicating that the diffusion is more affected by the shape of the initial distribution than by the location of the resonance zones. Small ($\langle \Delta n \rangle / \langle n \rangle \sim 1 - 10\%$), high-frequency (~ 1 MHz) fluctuations are observed to accompany this diffusion.

III. PARTICLE LOSS

There are three possible sources of plasma loss in a toroidal multipole: (1) recombination, (2) obstacles (including hoop supports), and (3) radial losses (hoop and wall). At the densities in the present experiment, recombination is negligible. Ionization causes the density to grow, and leads to a negative loss. For $kT_e \ll U_i$ (U_i is the ionization energy), as is the case late in the afterglow, ionization can be neglected. The particle loss to the supports was estimated by measuring the ion saturation current to a model support in the same relative position as a real support but electrically insulated from the hoop. The total current to the 12 real supports was taken as 12 times this current. The loss to the walls was measured by biasing all hoops and supports positive with respect to the wall and measuring the ion saturation current to the wall. The flux to the inner hoops was determined by biasing the upper and lower hoops as a floating double probe with mylar sleeves around the supports, and similarly for the outer hoops. These measurements parallel the more detailed tests made by Meade and Molvik³ for the gun injected plasma.

Figure 5 shows the relative loss for the various cases. The heating conditions are the same ($B_0 = 5$) as those for Fig. 4. Since the plasma is created near the inner hoops, the initial loss is primarily to the inner hoops. As time goes on, plasma moves toward the outer hoops until the magnetic field starts to decrease, at which time the hoop losses drop sharply, and plasma is transported out to the wall. At very

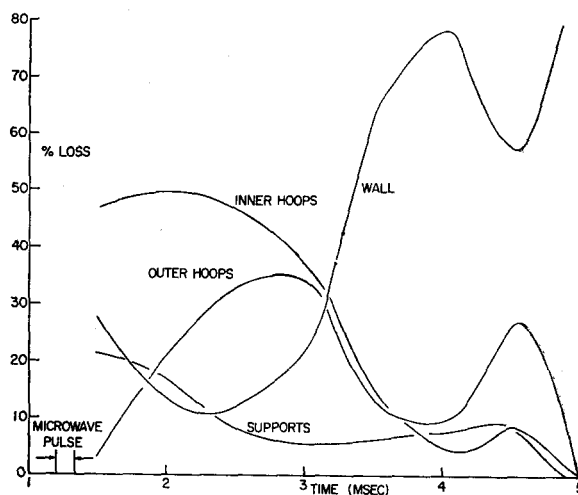


FIG. 5. Fractional loss of plasma to hoops, supports, and wall vs time after the beginning of the 5 msec multipole field pulse.

late times ($t > 4$ msec) the plasma has forgotten the manner in which it was created, and the fluxes to the hoops are approximately proportional to their relative areas. At peak magnetic field ($t = 2.25$ msec), the walls and supports each contribute about 10% of the total while the remaining 80% is lost to the hoops. These results are similar to those obtained for the gun plasma.³ Microwave plasmas with different density distributions give qualitatively similar results.

The plasma lifetime has been measured in three different ways: (1) The number of particles in the machine at time t can be determined by integrating the flux of particles to the hoops, supports, and wall from t to ∞ :

$$N(t) = \frac{1}{e} \int_t^{\infty} [I_H(t) + I_S(t) + I_W(t)] dt.$$

(2) A microwave cavity perturbation technique in which the entire cavity is filled with 24 GHz radiation can be used to measure the total number of electrons in the cavity by measuring the frequency shift δf of the cavity modes:

$$N(t) = \bar{n}(t) V = \frac{2\epsilon_0 m \omega^2 V}{e^2} \frac{\delta f}{f}.$$

(3) A Langmuir probe can be used to measure ion saturation current and electron temperature vs ψ and t , and the number of particles calculated from

$$N(t) = eA(2\pi M)^{1/2} \int_{-s}^s \frac{I_{0i}}{(kT_e)^{1/2}}(\psi, t) V'(\psi) d\psi.$$

The first two techniques were tried for a case resembling that discussed earlier ($B_0 = 5$), except

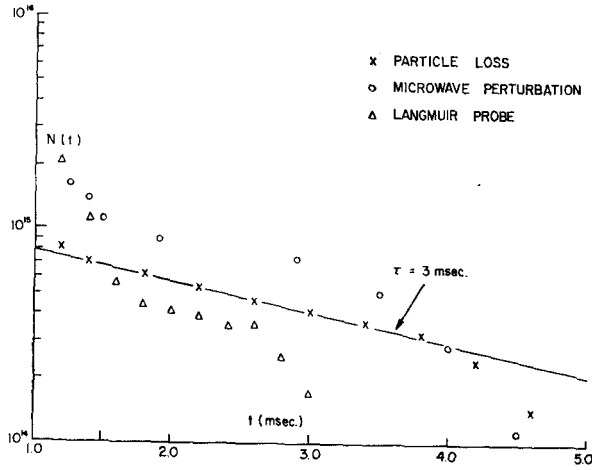


FIG. 6. Number of particles in the toroid vs time as measured by three different methods.

using the 3250 MHz system. The results are shown in Fig. 6. The Langmuir probe measurements in Fig. 6 were taken only on the separatrix, and this fact probably accounts for the rapid decay at late times. All methods indicate an initial rapid decay followed by a slower decay near peak field (2.25 msec), and then a rapid decay as the field dies away. The decay rate near peak field gives a lifetime of 3 msec, or about three times longer than the lifetime of the gun plasma as measured by the same methods.

The observed lifetime is somewhat longer than the lifetime calculated for Bohm diffusion, and seems to remain fairly constant over several milliseconds in spite of the rapid decay of electron temperature (see next section). The lifetimes do not appear to scale with ion temperature in a manner that would be consistent with thermal flow to the hoop supports, since even if the sheath criterion is taken into account, the microwave plasma lifetime should exceed the gun plasma lifetime by a factor of $[T_i(\text{gun})/T_e(\text{microwave})]^{1/2} \simeq 6$.

IV. ELECTRON COOLING

The electron temperature on the $B = 0$ axis was determined by the admittance probe method⁸ which consists of measuring the ion saturation current and the slope of probe I - V characteristic at the floating potential (V_f) by means of a balanced rf capacitance bridge. The electron temperature is then given by

$$\frac{kT_e}{e} = -I_{0i} \left. \frac{dV}{dI} \right|_{V_f}$$

The admittance probe, like the floating double probe⁹ and triple probe,¹⁰ suffers from the disadvantage that only the tail of the distribution is

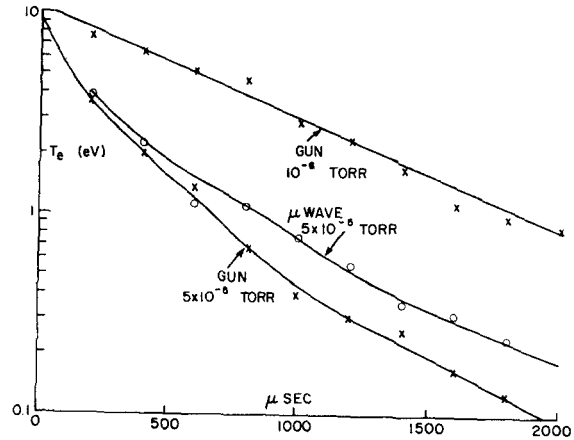


FIG. 7. Electron temperature for the gun and microwave plasma as measured by an admittance probe on the $B = 0$ axis vs time after injection.

sampled. However, the admittance probe has given agreement with swept single probes and electrostatic energy analyzers in cases where comparisons have been made.¹¹

Measurements of the electron temperature for both the gun and microwave plasma are shown in Fig. 7. The gun plasma temperature decay is approximately exponential in time with an initial value of ~ 10 eV and a decay time of ~ 1 msec. The temperature for the microwave case decays much faster. When the background pressure for the gun plasma is raised to a value equal to that used for the microwaves (5×10^{-5} Torr), the decay is much faster than at 10^{-6} Torr, suggesting that the fast decay for the microwave plasma is due primarily to the higher pressure.

The slight difference between the two high-pressure cases is well accounted for by the fact that the gun plasma is produced 700 μ sec later than the microwave plasma with respect to the confining magnetic field pulse, and hence some cooling due to magnetic field expansion is expected for the gun plasma. If we assume that the density distribution remains fixed in space while the field changes, and that the electron motion is adiabatic (i.e., $W_{\perp}/B = \text{const}$), the cooling rate for a sinusoidal magnetic field is given by

$$\frac{dT_e}{dt} = \frac{T_e}{B(t)} \frac{dB}{dt} = \frac{T_e}{\sin \omega t} \omega \cos \omega t = \omega T_e \cot \omega t$$

In order to further study the cooling mechanism, the temperature of the gun plasma 1 msec after injection was measured as a function of background gas pressure. The result is shown in Fig. 8. For low pressures, the temperature is relatively constant, but above about 10^{-6} Torr the decay rate is quite

sensitive to pressure. These observations suggest that the predominant cooling mechanism is different for the two plasmas. The strong pressure dependence at high pressures suggests that ionization and excitation of the background gas are important. Large light signals from photosensitive probes at high pressures support this hypothesis. Quantitative comparison of the observed cooling with the cooling calculated from electron-neutral, inelastic collision cross sections is difficult because of the importance of high- z impurities which are present in unknown quantities.

At low pressure, the exponential decay of temperature and relative insensitivity to pressure of the gun plasma suggest cooling due to the preferential loss of energetic electrons to obstacles in the plasma. Following a calculation by Lovberg¹² for the heat flux to an insulator or floating conductor in the plasma, the energy lost by electrons is given by

$$\begin{aligned} \frac{d}{dt} \left(\frac{3}{2} N k T_e \right) &= -\frac{1}{2} n \bar{v}_i A [e(V_p - V_f) + 2kT_e] \\ &\simeq -1.45 n \bar{v}_i A k T_e. \end{aligned}$$

The corresponding particle loss is given by

$$\frac{dN}{dt} = -\frac{1}{2} n \bar{v}_i A,$$

so that the cooling rate is

$$\frac{dT_e}{dt} \simeq -0.72 n \bar{v}_i A \left(\frac{T_e}{N} \right),$$

or about three times faster than the particle loss rate. From the observed decay of electron temperature for the gun plasma, the calculated cross section for loss is $\sim 65 \text{ cm}^2$ in reasonable agreement with the geometrical area of the probes and hoop supports.

The particle decay rate is comparable to, rather than three times slower than, the temperature decay rate, indicating that the loss of gun plasma cannot be totally accounted for by the thermal flow of ions to the hoop supports. Furthermore, the floating potential for both the gun and microwave plasma differs by several volts from the potential of the supports in contradiction to what would be expected for simple support losses.

Admittance probe measurements are subject to considerable error if the distribution departs slightly from a Maxwellian. The electron thermalization time as given by Spitzer¹³ is $650 \mu\text{sec}$ for $kT_e = 10 \text{ eV}$ and $n = 10^9 \text{ cm}^{-3}$. For the microwave plasma with

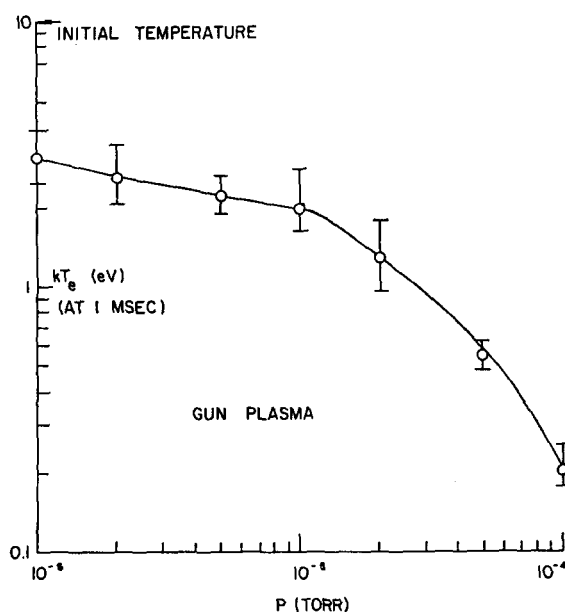


FIG. 8. Electron temperature of the gun injected plasma 1 msec after injection vs background hydrogen gas pressure.

$kT_e < 10 \text{ eV}$ and $n > 10^9 \text{ cm}^{-3}$, the approach to thermal equilibrium should be even faster.

V. FLUCTUATIONS

A. Between ψ_{crit} and the Wall

Simple magnetohydrodynamic theory predicts interchange instability in regions where

$$p'V'' = \frac{dp}{d\psi} \frac{d}{d\psi} \oint \frac{dl}{B} < 0.$$

This condition is satisfied between $\psi = \psi_{\text{crit}} = 3$ and the wall ($\psi = 5$). Large ($\delta V_f \sim kT_e/e$), $k_{\parallel} = 0$ fluctuations in floating potential are observed in this region as shown in Fig. 3(d). The oscillations are at a frequency of a few tens of kilohertz, and the density and potential fluctuations are approximately 180° out of phase implying small diffusion. Figure 9 shows how the amplitude of the density fluctuations varies with distance from the wall in the midplane. The fluctuations amount to about 40% in the unstable region and fall off rapidly inside ψ_{crit} . A similar behavior has previously been observed^{2,14} for the gun injected plasma, as shown by the dotted line in Fig. 9. When a toroidal magnetic field of 180 G is superimposed on the poloidal field, producing a stellaratorlike field with large rotational transform and shear, the amplitude of the fluctuations decreases in the originally unstable region and increases in the originally stable region in a manner similar to that previously observed for

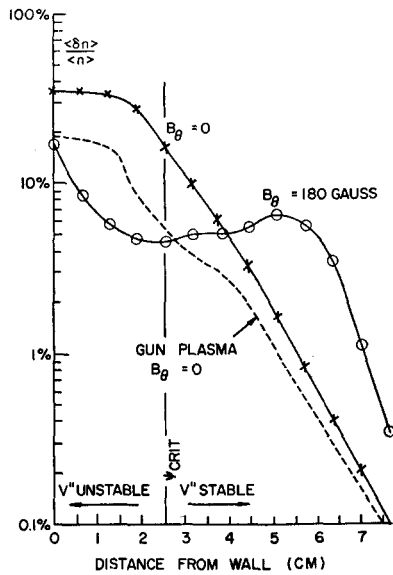


FIG. 9. Amplitude of density fluctuations in the 10–500 kHz range in the midplane near the wall where the plasma is expected to be interchange unstable.

the gun plasma.² The fluctuations are especially large in the region of zero average shear, 4.5 cm from the wall.

B. Fluctuations in Regions of Inverted Density Gradient

Interchange instabilities can also occur inside ψ_{crit} when the plasma pressure has a maximum strongly peaked off the separatrix. It has already been pointed out that this condition occurs when the plasma is generated, and Fig. 3(b) shows an example of the low-frequency fluctuation that results. This fluctuation has an amplitude of about 10 V/cm. Note that $E_\theta > 0$ for the first 60 μ sec causing plasma to $\mathbf{E} \times \mathbf{B}$ drift toward the wall initially at this azimuth, but as the density builds up [Fig. 3(a)] the electric field reverses and the plasma drifts towards the center with a velocity ($\sim 10^6$ cm/sec) that is consistent with the observed collapse of the density profile (Fig. 3).

Inverted density gradients can also arise when the magnetic field changes and moves the density peak off the separatrix. The oscilloscope trace in Fig. 4 shows an example of the fluctuations that occur on the $B = 0$ axis under these conditions. The plasma is produced while the field is still rising so that as the density distribution, which is initially peaked on the separatrix, moves toward the hoops, a large fluctuation appears. Near peak magnetic field, the fluctuation disappears, only to reappear later as the field decays and carries plasma out toward the wall. These fluctuations are similar to cases previously observed for the gun plasma,²

and may account for some of the diffusion observed in the density profiles in Fig. 4.

C. Fluctuations in Regions of Unfavorable Curvature

When the density gradient is sufficiently large, fluctuations appear in the magnetohydrodynamic stable region where the local field curvature is unfavorable. Figure 10 shows that the amplitude of these fluctuations is maximum where the density gradient is maximum and amounts to about a 10% variation in density. The fluctuations occur only on the side of the peak toward the wall and have nodes in the regions of favorable curvature. This drift wave propagates in the direction of the diamagnetic current and has a perpendicular wavelength of ~ 3 cm in agreement with the theoretical prediction^{15,16} of

$$k_\perp^2 \rho_i^2 \simeq \frac{T_i}{T_e},$$

where ρ_i is the ion gyroradius. The oscillation has a frequency of ~ 100 kHz in agreement with the prediction of

$$\omega \simeq 0.3 k_\perp \frac{k T_e}{e B} \left| \frac{\nabla n}{n} \right|,$$

and a parallel wavelength one-half as long as a closed field line. To a close approximation, the density and potential fluctuations are in phase implying no transport in agreement with the fact that the density gradient persists throughout the life of the plasma. The frequency and amplitude of the oscillations decrease in time as the electron temperature decays. The addition of a toroidal magnetic field of about 100 G does not suppress the fluctuations. The parallel phase velocity of the

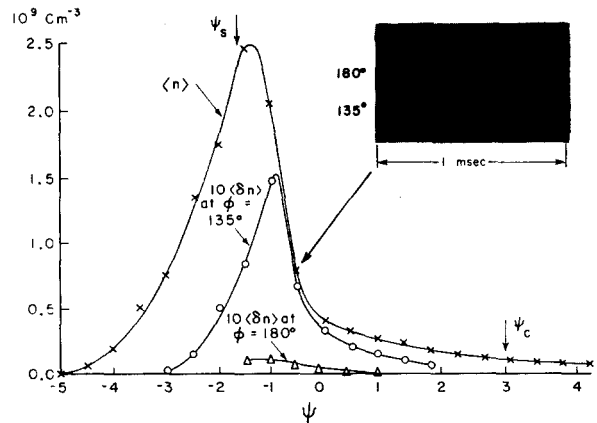


FIG. 10. Profile of density and amplitude of density fluctuations at 500 μ sec showing evidence of drift waves localized in the region of unfavorable curvature.

wave is greater than the ion thermal speed and less than the electron thermal speed:

$$\bar{v}_i < \frac{\omega}{k_{\parallel}} < \bar{v}_e.$$

This wave is apparently identical to the collisionless ballooning mode observed by Meade and Yoshikawa¹⁷ in a linear quadrupole.

D. Fluctuations between the Separatrix and the Hoops

Perhaps the most unsettling observation of the microwave produced plasma is the rapid diffusion toward the hoops, as seen for example in Fig. 2. There are a minimum of 20 ion gyroradii between the separatrix and the hoops. This motion is sometimes accompanied by fluctuations as in Fig. 3(e). This region has only favorable curvature and should be stable according to any simple theory. It has already been pointed out that the loss is present irrespective of the position of the resonance zones, although the appearance of the fluctuations varies drastically. In fact, some cases have been observed in which the loss is present without noticeable fluctuations. Since hoop losses constitute the major source of plasma loss in this experiment, as well as for the gun injected plasma, the mechanism which produces this loss is worthy of further study. It is possible that azimuthally asymmetric initial density distributions or localized perturbations such as the hoop supports or diagnostic and pump ports generate low-frequency electric fields which form convective cells enabling the plasma to move out toward the walls and hoops.^{18,19}

VI. CONCLUSIONS

It has been shown that a cold ion plasma can be produced in a toroidal octupole by raising the background gas pressure to $\sim 10^{-4}$ Torr and injecting microwave power (10–100 kW) at a frequency such that electron cyclotron resonance occurs somewhere within the cavity. The behavior of the resulting afterglow plasma is similar to that of a hot ion plasma produced by gun injection except the particle loss rate is slower and the temperature decay rate is faster. By changing the microwave frequency and magnetic field strength, a variety of density distributions can be produced. These distributions change in time as a result of inductive electric fields caused by the time varying magnetic field and fluctuating electric fields due to instabilities. Some diffusion is observed when $\dot{B} = 0$ and no fluctua-

tions are present, however, indicating that some additional unknown mechanism is responsible for the fact that $\sim 80\%$ of the plasma is lost to the hoops.

ACKNOWLEDGMENTS

I am grateful to Professor D. W. Kerst for his supervision and interest in this work. Professor D. M. Meade also contributed much helpful discussion. The sharing of ideas, data, and equipment with Dr. J. A. Schmidt, Dr. D. E. Lencioni, Dr. G. W. Kuswa, and A. W. Molvik was very helpful. P. Nonn constructed the microwave systems.

Financial support was provided by the United States Atomic Energy Commission.

* Part of a thesis submitted in partial fulfillment of the requirements for the degree of Ph.D. at the University of Wisconsin.

¹ R. A. Dory, D. W. Kerst, D. M. Meade, W. E. Wilson, and C. W. Erickson, *Phys. Fluids* **9**, 997 (1966).

² D. E. Lencioni, J. W. Poukey, J. A. Schmidt, J. C. Sprott, and C. W. Erickson, *Phys. Fluids* **11**, 1115 (1968).

³ H. Forsen, D. Kerst, D. Lencioni, D. Meade, F. Mills, A. Molvik, J. Schmidt, J. Sprott, and K. Symon, in *Plasma Physics and Controlled Nuclear Fusion Research* (International Atomic Energy Agency, Vienna, 1969), Vol. I, p. 313.

⁴ T. Ohkawa, M. Yoshikawa, and A. A. Schupp, in *Plasma Physics and Controlled Nuclear Fusion Research* (International Atomic Energy Agency, Vienna, 1969), Vol. I, p. 329. C. W. Erickson, G. v. Gierke, G. Grieger, F. Rau, and H. Wobig, in *Plasma Physics and Controlled Nuclear Fusion Research* (International Atomic Energy Agency, Vienna, 1969), Vol. I, p. 339. M. Roberts, I. Alexeff, R. A. Dory, W. Halchin, and W. L. Stirling, in *Plasma Physics and Controlled Nuclear Fusion Research* (International Atomic Energy Agency, Vienna, 1969), Vol. I, p. 351. S. Yoshikawa, M. Barault, W. Harries, D. Meade, R. Palladino, and S. von Goeler, in *Plasma Physics and Controlled Nuclear Fusion Research* (International Atomic Energy Agency, Vienna, 1969), Vol. I, p. 403. A. F. Kuckes and R. B. Turner, in *Plasma Physics and Controlled Nuclear Fusion Research* (International Atomic Energy Agency, Vienna, 1969), Vol. I, p. 329. O. A. Anderson, D. H. Birdsall, C. W. Hartman, and E. J. Lauer, in *Plasma Physics and Controlled Nuclear Fusion Research* (International Atomic Energy Agency, Vienna, 1969), Vol. I, p. 443.

⁵ J. C. Sprott (to be published).

⁶ M. N. Rosenbluth and C. L. Longmire, *Ann. Phys. (N. Y.)* **1**, 120 (1957).

⁷ D. E. Lencioni, Ph.D. thesis, University of Wisconsin (1969).

⁸ J. C. Sprott, *Rev. Sci. Instr.* **39**, 1569 (1968).

⁹ E. O. Johnson and L. Malter, *Phys. Rev.* **80**, 58 (1950).

¹⁰ S. Chen and T. Sekiguchi, *J. Appl. Phys.* **36**, 2363 (1965).

¹¹ D. M. Meade and G. W. Kuswa (private communication).

¹² R. H. Lovberg, in *Plasma Diagnostic Techniques*, edited by R. H. Huddleston and S. L. Leonard (Academic, New York, 1965), p. 95.

¹³ L. Spitzer, Jr., *Physics of Fully Ionized Gases* (Interscience, New York, 1962), 2nd ed., p. 133.

¹⁴ D. M. Meade, *Phys. Rev. Letters* **17**, 677 (1966).

¹⁵ N. A. Krall and M. N. Rosenbluth, *Phys. Fluids* **8**, 1488 (1965).

¹⁶ S. Yoshikawa, *Bull. Am. Phys. Soc.* **12**, 630 (1967).

¹⁷ D. M. Meade and S. Yoshikawa, *Phys. Fluids* **10**, 2649 (1967).

¹⁸ J. A. Schmidt, Ph.D. thesis, University of Wisconsin (1969).

¹⁹ G. O. Barney and J. C. Sprott, *Phys. Fluids* **12**, 707 (1969).